Stable Au25(SR)18/TiO2 Composite Nanostructure with Enhanced Visible Light Photocatalytic Activity

ARTICLE *in* JOURNAL OF PHYSICAL CHEMISTRY LETTERS · AUGUST 2013

Impact Factor: 7.46 · DOI: 10.1021/jz401447w

5 AUTHORS, INCLUDING:

Changlin Changlin
Jiangxi University of Science and Technology
1 PUBLICATION **49** CITATIONS
SEE PROFILE

Gao Li
Dalian Institute of Chemical Physics
47 PUBLICATIONS **1,219** CITATIONS
SEE PROFILE

Hideya Kawasaki
Kansai University
154 PUBLICATIONS **2,827** CITATIONS
SEE PROFILE

THE JOURNAL OF PHYSICAL CHEMISTRY Letters

Letter

pubs.acs.org/JPCL

Stable $Au_{25}(SR)_{18}/TiO_2$ Composite Nanostructure with Enhanced Visible Light Photocatalytic Activity

Changlin Yu,*[,†,‡] Gao Li,[‡] Santosh Kumar,[‡] Hideya Kawasaki,[‡] and Rongchao Jin*[,‡]

[†]School of Metallurgy and Chemical Engineering, Jiangxi University of Science and Technology, 86 Hongqi Road, Ganzhou 341000, Jiangxi, People's Republic of China

[‡]Department of Chemistry, Carnegie Mellon University, Pittsburgh, Pennsylvania 15213, United States

Supporting Information

ABSTRACT: We report the visible light photocatalytic properties of a composite material consisting of $Au_{25}(SR)_{18}$ nanoclusters (R:CH_2CH_2Ph) and TiO_2 nanocrystals. The effects of $Au_{25}(SR)_{18}$ nanoclusters on the photocatalytic activity of TiO_2 nanocrystals were evaluated in the reaction of photocatalytic degradation of methyl orange. The loading of $Au_{25}(SR)_{18}$ nanoclusters onto TiO_2 results in strong visible light absorption by the composite and, more importantly, a 1.6 times increase in visible light photocatalytic activity. Furthermore, the $Au_{25}(SR)_{18}/TiO_2$ composite nanostructure exhibits high stability in recycling tests. The $Au_{25}(SR)_{18}$ nanolusters dispersed on the TiO_2 surface can act as a small-band-gap semiconductor to absorb visible light, giving rise to electron−hole separation and producing singlet oxygen ($^1O_2$). Both the generated hydroxyl radicals ($HO^•$) and $^1O_2$ are rationalized to be responsible for the decomposition of the dye.

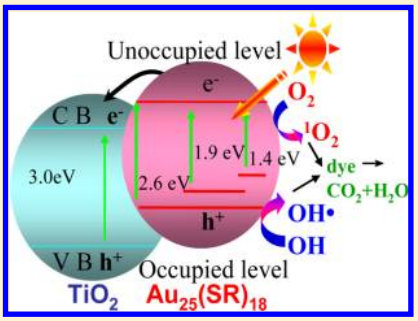

SECTION: Surfaces, Interfaces, Porous Materials, and Catalysis

Recently, gold nanoparticles (AuNPs) have stimulated tremendous research interest in photocatalysis.[1−6] Under light irradiation, metallic AuNPs (typically >2 nm) exhibit localized surface plasmon resonance(s).[7] Such plasmon excitation enables plasmon-enhanced photocatalysis.[8−11] On the other hand, when the AuNPs fall in the extremely small size regime (<2 nm), drastic changes occur to the atom packing structure[12−14] as well as their optical properties.[15−19] This new class of atomically precise nanoparticles is often called nanoclusters in order to distinguish them from plasmonic AuNPs. Among the reported gold nanoclusters, Au_{25} (1.3 nm) is very robust and exhibits some unique properties such as one-electron transitions in the visible absorption spectrum[13,17] and fluorescence.[15,16] Tatsuma et al.[20,21] reported that TiO_2 electrodes modified by glutathione (SG)-protected Au_{25} nanoclusters could exhibit anodic photocurrents and negative photopotential shifts in response to visible and near-infrared (NIR) light in the presence of appropriate electron donors. The photoexcited electrons in $Au_{25}(SG)_{18}$ can be utilized to reduce Ag^+, Cu^{2+}, and dissolved oxygen.[20] Lee et al.[22] found that SG-protected AuNPs (e.g., 2.8 nm) in Au/ZnO composites could store the excited electrons from ZnO and enhance the charge separation, which benefits the oxidative degradation of rhodamine 6G. Our previous work[13] showed that thiolate-protected Au_{25} nanoclusters possess a distinct HOMO−LUMO gap, $E_g \approx 1.3$ eV. These nanoclusters are also extraordinarily robust against excess thiol etching.[17] The new class of atomically precise gold nanoclusters can catalyze a number of reactions,[23] such as photocatalysis,[20,22] selective oxidation of sulfide to sulfoxide,[24] and carbon monoxide oxidation at mild temperatures,[25] and thus holds great potential in catalysis research, especially in correlating the catalytic properties with the cluster structure.[23]

With respect to the photocatalytic materials, TiO_2 is the most widely used photocatalyst in self-cleaning and removal of hazardous compounds due to its superior photocatalytic activity, chemical stability, low cost, and nontoxicity.[26−31] However, a major drawback of TiO_2 is its large band gap (3.2 eV), and thus, only UV light, which constitutes merely 2−3% of the solar spectrum, can be utilized, which significantly limits the use of solar light in photocatalysis.

Herein, we investigate the extraordinary effects of $Au_{25}(SR)_{18}$ nanoclusters on the photocatalytic activity of nanocrystalline TiO_2 under different light irradiation (UV and visible). Our research demonstrates that loading a small amount (~1%) of $Au_{25}(SR)_{18}$ nanoclusters onto TiO_2 can substantially increase the visible light activity of TiO_2.

The synthesis of $Au_{25}(SCH_2CH_2Ph)_{18}$ nanoclusters followed a previously reported method.[13] The X-ray structure of $Au_{25}(SCH_2CH_2Ph)_{18}$ exhibits a core−shell-type structure irrespective of the charge state,[32] which consists of a Au_{13} icosahedral core encapsulated by an exterior, nonclosed Au_{12} shell (Figure 1a), and the entire cluster is protected by 18 thiolate ligands. The phase composition and the crystallinity of the $Au_{25}(SR)_{18}/TiO_2$ composite were characterized by powder X-ray diffraction (XRD). As shown in Figure 1b, the TiO_2

Received: July 11, 2013
Accepted: August 6, 2013

   dx.doi.org/10.1021/jz401447w | J. Phys. Chem. Lett. 2013, 4, 2847−2852

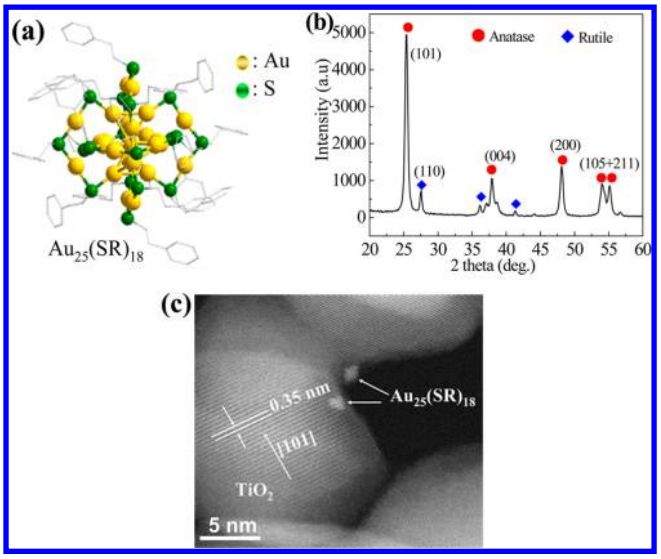

Figure 1. (a) Total structure of $Au_{25}(SCH_2CH_2Ph)_{18}$ nanoclusters. (b) The XRD pattern of $Au_{25}(SR)_{18}/TiO_2$; only the TiO_2 diffraction peaks are observable. (c) The high-resolution STEM image of $Au_{25}(SR)_{18}/TiO_2$.

nanocrystals comprise two phases, anatase and rutile. The five strong diffraction peaks at 2θ of 25.3, 38.2, 48.1, 53.5, and 55.6° are attributed to anatase-TiO_2 (JCPDF84-1285), and weak peaks at 27.5, 36.2, and 41.3° are attributed to rutile-TiO_2, as indexed in Figure 1b. These strong and sharp diffraction peaks demonstrate the high crystallinity of TiO_2 (15−25 nm). The average crystallite size of TiO_2 is determined by the Scherrer equation, $D = 0.89\lambda/B(2\theta)\cos\theta$, where $B(2\theta)$ is the width of the XRD peak at half height (in radian), λ is the wavelength of the X-ray (λ = 0.154 nm), θ is the angle between the incident and diffracted beams in degrees, and D is the average crystallite size of the TiO_2 powder in nanometers. The strongest plane, that is, {101}, was used in the calculation. The as-obtained average crystalline size is about 20 nm. Of note, no diffraction peaks of $Au_{25}(SR)_{18}$ were observed in the composite due to the very low content (~0.94%) and peak broadening caused by the ultrasmall size of Au_{25} (1.3 nm).[33] High-resolution scanning transmission electron microscopy (STEM) was performed to image the loaded $Au_{25}(SR)_{18}$ nanoclusters (Figure 1c). The ultrasmall, 1.3 nm, Au_{25} nanoclusters were clearly observed (Figure 1c), confirming that $Au_{25}(SR)_{18}$ nanoclusters were successfully loaded on TiO_2. In addition, STEM shows the faceted TiO_2 nanocrystals with a size of ~20 nm, consistent with the XRD result. The interplanar distance is about 0.35 nm, in agreement with the {101} plane of the anatase phase of TiO_2.

The UV−vis absorption spectra of the samples were further measured. The $Au_{25}(SR)_{18}$ nanoclusters in dichloromethane show absorption bands at 400, 445, 670, and 800 nm (Figure 2a1), which are characteristic of Au_{25} nanoclusters.[32−36] Figure 2a2 shows the absorption spectrum on the photon energy scale, with the three bands at 1.8, 2.8, and 3.1 eV. Due to strong quantum size effects, the Au_{25} nanocluster shows multiple molecular-like *single-electron* transitions in its optical absorption spectrum,[13] as opposed to the *collective electron* excitation (i.e., plasmon) in conventional AuNPs. Figure 2b1 shows that the

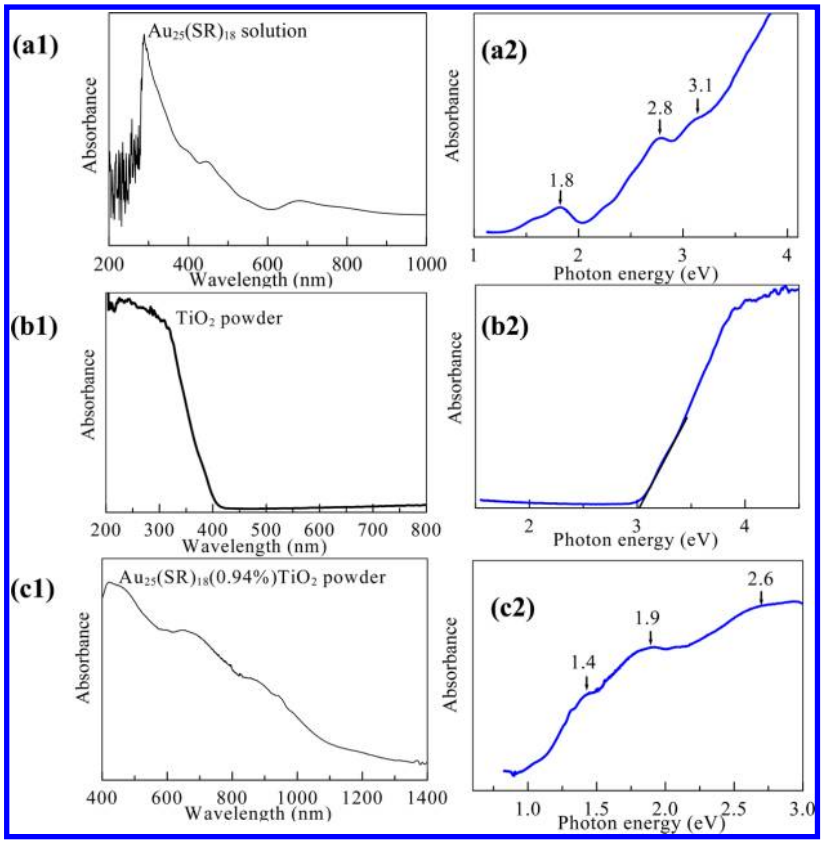

Figure 2. UV−vis absorption spectra of the samples, (a1, a2) $Au_{25}(SR)_{18}$ in dichloromethane; UV−vis diffuse reflectance spectra of TiO_2 (b1, b2) and $Au_{25}(SR)_{18}$(0.94%)/TiO_2 (c1, c2). In panel (a1), the precipitous drop in absorbance below ~300 nm is caused by solvent cutoff.

dx.doi.org/10.1021/jz401447w | J. Phys. Chem. Lett. 2013, 4, 2847−2852

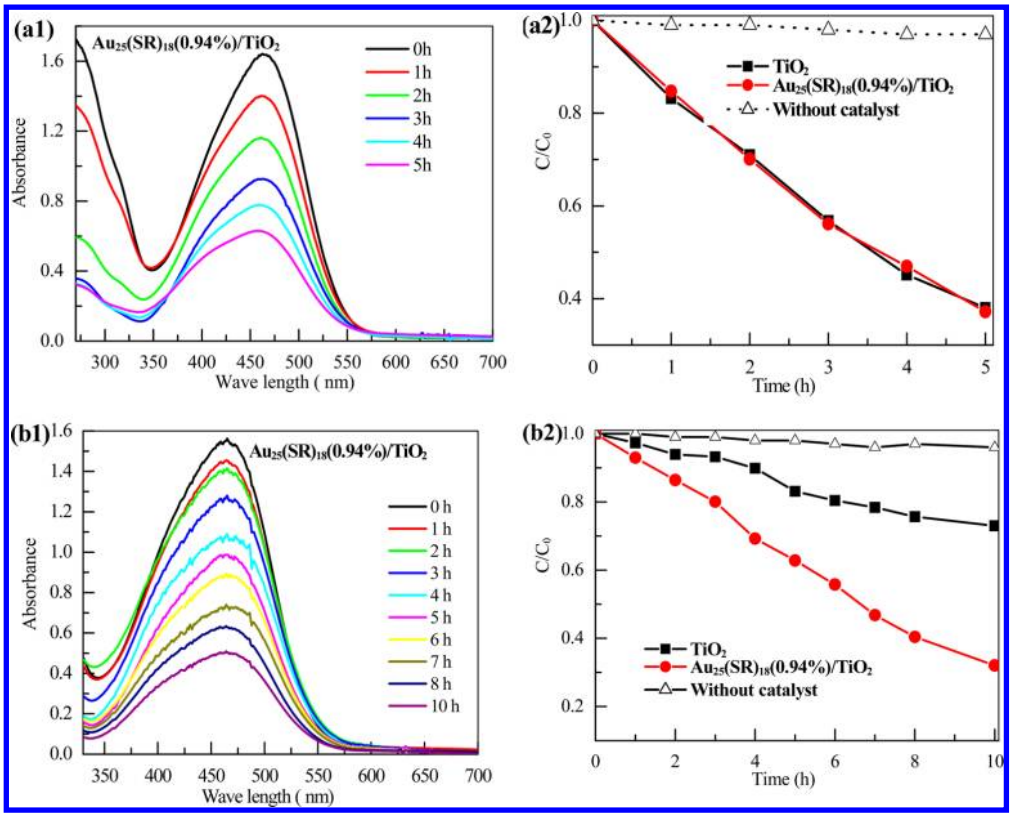

Figure 3. The effect of $Au_{25}(SR)_{18}$ nanoclusters on the photocatalytic activity of TiO_2 under UV light or visible light irradiation. (a1, b1) Spectral changes of methyl orange as a function of irradiation time and (a2, b2) changes of methyl orange concentration under UV and visible light, respectively.

absorption edge of pure nanocrystalline TiO_2 is around 400 nm, corresponding to a band gap of 3.1 eV. The loading of $Au_{25}(SR)_{18}$ nanoclusters results in a substantial red shift of the absorption of the $Au_{25}(SR)_{18}(0.94\%)/TiO_2$ composite, and absorption bands at 440, 670, and 870 nm appear (Figure 2c1). The 400 nm peak of solution-phase $Au_{25}(SR)_{18}$ nanoclusters is smeared out in the $Au_{25}(SR)_{18}/TiO_2$ composite because this peak is close to the band gap position of TiO_2, but the 440 and 670 nm peaks are retained. The 870 nm peak of the $Au_{25}(SR)_{18}/TiO_2$ composite corresponds to the ~800 nm band of unsupported $Au_{25}(SR)_{18}$. The slight red shift (~0.12 eV) should be caused by the interaction between the cluster and TiO_2. It is worth noting that the ~800 nm broad peak of unsupported $Au_{25}(SR)_{18}$ is quite sensitive to changes such as charge state[32] and other factors. The $Au_{25}(SR)_{18}$ clusters are stable, and no size change was observed in wet deposition of them onto TiO_2. Our STEM analysis confirmed that the size of $Au_{25}(SR)_{18}$ nanoclusters (1.3 nm) remains unchanged. The UV−vis diffuse reflectance spectrum suggests that this composite nanostructure has intense light absorption in both the visible and NIR regions. On the photon energy scale (Figure 2c2), three absorption bands are observed at ~1.4, 1.9, and 2.6 eV. Compared with the absorption spectrum of pure Au_{25} nanoclusters, the visible and NIR absorption bands of the composite originate from the loaded Au_{25} nanoclusters.

Degradation of methyl orange under UV and visible light, respectively, was measured to investigate the effects of $Au_{25}(SR)_{18}$ nanoclusters on the TiO_2 photocatalytic performance. Figure 3a1 shows the typical temporal evolution of the dye's spectral changes during the UV irradiation (365 nm) in the presence of $Au_{25}(SR)_{18}(0.94\%)/TiO_2$. It shows that the intensity of the 463 nm adsorption peak of methyl orange decreases gradually, which indicates that the catalyst exhibits photocatalytic activity. The blank test confirms that without the catalyst, methyl orange cannot be degraded under UV light, indicating that methyl orange is a stable molecule and its photolysis is negligible. When comparing the catalytic activities of pure TiO_2 (i.e., without $Au_{25}(SR)_{18}$) and $Au_{25}(SR)_{18}(0.94\%)/TiO_2$, no distinct difference in UV photocatalytic activity was found (Figure 3a2), suggesting that the $Au_{25}(SR)_{18}$ nanoclusters show no distinct effect under UV light.

Interestingly, under visible light irradiation, $Au_{25}(SR)_{18}$ nanoclusters substantially increase the photocatalytic activity (Figure 3b1 and b2). Here, we define $D = (C_0 - C)/C_0$ (where D is the decomposition ratio and C_0 is the initial concentration of methyl orange). After 10 h of visible light irradiation, the values of D over TiO_2 and $Au_{25}(SR)_{18}(0.94\%)/TiO_2$ are 27% and 69%, respectively; thus, $Au_{25}(SR)_{18}$ nanoclusters largely increase the visible photocatalytic activity. A small loading (0.94% $Au_{25}(SR)_{18}$ nanoclusters) on TiO_2 brings about a net 1.6 times increase in the photocatalytic activity of the composite. Usually, there are three possible reaction mechanisms for the dye degradation under visible light irradiation, a photolysis process, a dye photosensitization process,[37,38] and a photocatalytic process. The dye photosensitization mechanism is closely related to the properties of the dye, such as the structural stability of the dye. Figure 3b2 indicates that methyl orange can only be slightly degraded under visible light irradiation without catalysts, indicating that methyl orange is a stable molecule and the photolysis can be ignored. In addition, our experimental data on the methyl orange decolorization with pure anatase TiO_2 as the catalyst shows that the dye

dx.doi.org/10.1021/jz401447w | J. Phys. Chem. Lett. 2013, 4, 2847−2852

photosensitization process can be ignored. To test the stability of $Au_{25}(SR)_{18}(0.94\%)/TiO_2$, recycling tests were further carried out. The reacted catalysts were separated by high speed centrifuging (15000 rpm). The separated catalysts were dried in vacuum at 100 °C for 12 h and then used again. In the three recycling tests, the degradation rate of the dye was maintained at around 50% (see Supporting Information Figure S1). This indicates that this composite nanostructure shows very good stability.

As for the different influences of $Au_{25}(SR)_{18}$ in the UV and visible light activity tests, we propose the following mechanisms. Under UV light irradiation, no obvious increase in photocatalytic activity occurred with $Au_{25}(SR)_{18}$ present on TiO_2, indicating that the $Au_{25}(SR)_{18}$ nanocluster cannot act as an efficient electron trap to facilitate the electron−hole separation in TiO_2, which is consistent with the report by Lee and co-workers;[22] in their studies, Au_{25} was found to exhibit low efficiency in promoting the electron−hole separation in ZnO. Moreover, in our case the $Au_{25}(SR)_{18}$ content is very low (0.94%wt). Our previous density functional theory calculations for the electronic structure and optical absorption spectrum of $Au_{25}(SR)_{18}$ showed a discrete electronic structure and a HOMO−LUMO gap of $E_g \approx 1.3$ eV.[13] Therefore, $Au_{25}(SR)_{18}$ nanoclusters are more like a semiconductor with a small band gap, rather than the metallic state. The loading of a small amount of $Au_{25}(SR)_{18}$ nanoclusters can not produce obvious effects in UV light photocatalytic activity.

On the other hand, under visible light irradiation, TiO_2 only has weak photodegradation activity due to the weak absorption of rutile TiO_2 at ~400 nm. Loading 0.94% $Au_{25}(SR)_{18}$ nanoclusters onto TiO_2 largely increases the visible light photocatalytic activity. The enhancing mechanism of $Au_{25}(SR)_{18}$ nanoclusters is illustrated in Figure 4. According

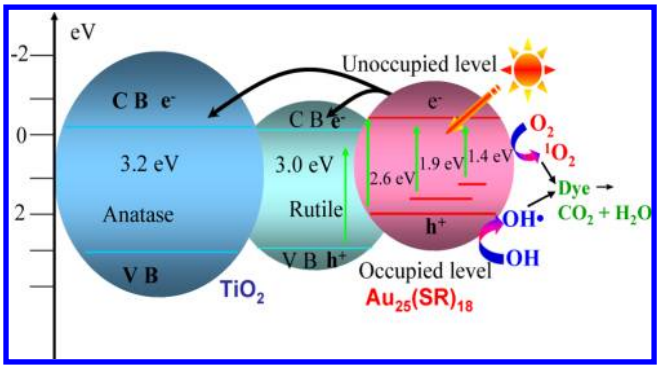

Figure 4. The photocatalytic mechanisms of $Au_{25}(SR)_{18}/TiO_2$ under visible light irradiation.

to the Kohn−Sham molecular orbitals (MOs), the absorption peaks of $Au_{25}(SR)_{18}$ at 440, 670, and 870 nm are ascribed to the various electron transitions from the occupied levels to the unoccupied levels.[13,32] Under visible light irradiation, $Au_{25}(SR)_{18}$ nanoclusters are easily excited and correspondingly generate electrons and holes. The photogenerated electron in $Au_{25}(SR)_{18}$ can be injected into the conduction band (CB) of anatase and rutile TiO_2 because of the well-aligned energy bands and intimate contact as well as interaction between TiO_2 and $Au_{25}(SR)_{18}$. Tatsuma et al.[21] confirmed such an electron injection process in their test of the photocurrent action spectrum of the $Au_{25}(SG)_{18}$−TiO_2(anatase) electrode. In this test, the potentials for the lower edge of the TiO_2 (anatase) CB and the unoccupied level of $Au_{25}(SG)_{18}$ were respectively determined to be +0.1 and −0.1 V versus SHE. Our calculations (see the Supporting Information) indicate that the CB of rutile TiO_2 (−0.1 eV) is more positive than that of anatase TiO_2 (−0.2 eV). Therefore, it is reasonable to infer that in our system, the potential of $Au_{25}(SR)_{18}$ is more negative than the CB potentials of both anatase and rutile TiO_2, and the transfer of the photogenerated electrons from $Au_{25}(SR)_{18}$ to the CB of anatase and rutile TiO_2 can take place. In such a way, the photoinduced electrons and holes can be efficiently separated, and the recombination of electron−hole can be reduced. The produced holes can further transform to hydroxyl radicals ($HO^{\bullet}$), which are usually the mainly active species in dye degradation.[39−41]

More interestingly, over the supported $Au_{25}(SR)_{18}$, another mechanism may involve singlet oxygen ($^1O_2$) production under visible or NIR light irradiation and the role of $^1O_2$ in degrading the dye. Our recent studies found out that $Au_{25}(SR)_{18}$ had a high efficiency of $^1O_2$ generation under green light irradiation. The tests for TiO_2 and $Au_{25}(SR)_{18}/TiO_2$ in $^1O_2$ production are presented in Figure S2 (see the Supporting Information for details). Figure S2(a) (Supporting Information) shows that no $^1O_2$ was generated over TiO_2, whereas over $Au_{25}(SR)_{18}/TiO_2$ (Figure S2(b), Supporting Information), the 415 nm absorption band of 1,3-diphenylisobenzofuran (DPBF, a specific probe for $^1O_2$)[42] decreased during irradiation with 532 nm light, and there was a decrease in fluorescence of the DPBF (Figure S2(c), Supporting Information), suggesting $^1O_2$ production by $Au_{25}(SR)_{18}$. The generation of $^1O_2$ by $Au_{25}(SR)_{18}$ was attributed to an energy-transfer process after light absorption by $Au_{25}(SR)_{18}$. To test the visible light photocatalytic activity of unsupported Au_{25} clusters, we prepared captopril-protected $Au_{25}(Capt)_{18}$, which is soluble in water and has similar capability as $Au_{25}(SR)_{18}$ to produce singlet oxygen to degrade methyl orange. As shown in Figure S3 (Supporting Information), when methyl orange was mixed with $Au_{25}(Capt)_{18}$ and subjected to visible light irradiation, the 460 nm absorption peak of methyl orange decreased gradually, suggesting that methyl orange was degraded under Au_{25} catalysis. To verify the oxidation capability of $^1O_2$ in decomposing methyl orange, we further used basic blue 24 ($C_{18}H_{22}ClH_3S{\cdot}xZnCl_2$), a known dye for $^1O_2$ production, to produce $^1O_2$; we found that $^1O_2$ can quickly decompose methyl orange (see Figure S4, Supporting Information). Moreover, in the $Au_{25}(SR)_{18}/TiO_2$ photocatalytic reaction system, we added a trace amount of $^1O_2$ quencher, L-histidine; an obvious decrease in activity was observed (see Figure S5, Supporting Information). In contrast, the quenching effect by L-histidine was not observed over the plain TiO_2 catalyst. These results further provide evidence for the involvement of singlet oxygen in the photocatalytic degradation mechanism.

Taken together, the above two mechanisms (hydroxyl radicals and singlet oxygen productions) explain that even a small amount of $Au_{25}(SR)_{18}$ loading onto TiO_2 can largely enhance the visible light photocatalytic activity of the composite in decomposing the dye.

In summary, we have investigated the effects of $Au_{25}(SR)_{18}$ nanoclusters on the photocatalytic activity of nanocrystalline TiO_2. The loading of $Au_{25}(SR)_{18}$ nanoclusters onto TiO_2 gives rise to largely enhanced visible light photocatalytic activity of the $Au_{25}(SR)_{18}$ (0.94%)/TiO_2 composite. The influence of $Au_{25}(SR)_{18}$ on the photocatalytic activity depends on the light source. Under UV light irradiation, no influence was observed.

dx.doi.org/10.1021/jz401447w | J. Phys. Chem. Lett. 2013, 4, 2847−2852

However, in the visible light photocatalysis, the $Au_{25}(SR)_{18}$ nanocluster brings about a 1.6 times net increase in the photocatalytic activity. In addition, we have shown that $Au_{25}(SR)_{18}$ nanoclusters act as the role of a small-band-gap semiconductor and facilitate the electron−hole separation. The dispersed $Au_{25}(SR)_{18}$ nanoclusters could also produce $^1O_2$, which can participate in the decomposition of the dye. The $Au_{25}(SR)_{18}/TiO_2$ composite nanostructures are very stable under visible light irradiation. Our finding opens up a new avenue of utilizing Au_{25} nanoclusters as a new small-band-gap semiconductor for designing a visible-light-responsive composite photocatalyst and potentially other photoelectronic systems.

EXPERIMENTAL METHODS

All chemicals were purchased from Sigma-Aldrich

Synthesis of $Au_{25}(SR)_{18}$ Nanoclusters. The synthesis of $Au_{25}(SR)_{18}$ (R═CH_2CH_2Ph) nanoclusters followed a previously reported procedure.[13] Briefly, $HAuCl_4·3H_2O$ (0.2 mmol, dissolved in 5 mL of nanopure water) and tetraoctylammonium bromide (TOAB, 0.24 mmol dissolved in 10 mL of toluene) were combined in a 25 mL tri-neck round-bottom flask. The solution was vigorously stirred for 15 min, and the aqueous was then removed. Thiol ($HSCH_2CH_2Ph$, 0.6 mmol) was added to the flask, and stirring was reduced to a very slow speed (50 rpm). After the solution turned to clear (2 h), $NaBH_4$ (2 mmol, 5 mL of cold aqueous solution) was rapidly added all at once. After aging overnight, methanol was added to separate Au nanoclusters from TOAB and other side products. The $Au_{25}(SR)_{18}$ clusters were collected after removing the supernatant by rotary evaporation.

Synthesis of $Au_{25}(SR)_{18}/TiO_2$. Typically, 1 mg of $Au_{25}(SR)_{18}$ clusters was dissolved in 5 mL of dichloromethane (DCM), and 100 mg of TiO_2 powder was added. After stirring for 24 h at room temperature, the $Au_{25}(SR)_{18}/TiO_2$ powders were collected by centrifugation and dried at 120 °C in a vacuum oven. The as-obtained $Au_{25}(SR)_{18}/TiO_2$ powders showed a purple color. The final mass content of $Au_{25}(SR)_{18}$ over TiO_2 is about 0.94%, determined by thermogravimetric analysis (TGA) (see Figure S6, Supporting Information).

Characterization of the Catalyst. Powder XRD data were recorded on an X'Pert PRO X-ray diffractometer at 40 kV and 40 mA for monochromatized Cu K_α (λ = 1.5418 Å) radiation. A high-resolution transmission electron microscopy (HRTEM) image was recorded on a Tecnai 20 FEG microscope. UV−vis diffuse reflectance spectra were achieved using a UV−vis spectrophotometer (UV-2550, Shimadzu). The absorption spectra were referenced to $BaSO_4$.

Photocatalytic Activity Measurements. The effects of $Au_{25}(SR)_{18}$ nanoclusters on the photocatalytic performance of nanocrystalline TiO_2 were evaluated by measuring the degradation of the methyl orange in an aqueous solution under UV (365 nm) or visible light irradiation. In the UV light activity test, a 6 W, 365 nm UV lamp (UVLMS-38 EL Series Lamp) was used as the light source. The photocatalyst (0.05 g) was suspended in a 100 mL aqueous solution of methyl orange with the concentration of C_0 = 0.020 g/L. Prior to light illumination, the suspension was magnetically stirred for 40 min in the dark to attain an adsorption/desorption equilibrium. The suspension was vigorously stirred during the photocatalytic reaction process. At given time intervals of illumination, the reaction mixture was sampled. After centrifugation, the dye concentration was measured at the maximum absorption wavelength of the dye on a UV−vis spectrophotometer (Agilent, HP8453). In the visible light activity test, the experiment was similarly done, except a 150 W quartz halogen lamp (Fiber-Lite MI-150 illuminator) was used as the light source.

ASSOCIATED CONTENT

Supporting Information

Recycling tests of $Au_{25}(SR)_{18}(0.94\%)/TiO_2$ in the degradation of methyl orange, electronegativity calculation for the electronic band structure of anatase TiO_2 and rutile TiO_2, singlet oxygen production over $Au_{25}(SR)_{18}/TiO_2$ under 532 nm green light irradiation, singlet oxygen ($^1O_2$) decomposed methyl orange, the effect of a quencher (L-histidine) on the photocatalytic activity of $Au_{25}(SR)_{18}/TiO_2$, and TGA profiles of $Au_{25}(SR)_{18}(0.94\%)/TiO_2$ and plain TiO_2 in air atmosphere. This material is available free of charge via the Internet at http://pubs.acs.org.

AUTHOR INFORMATION

Corresponding Author

*E-mail: yuchanglinjx@163.com (C.Y.); rongchao@andrew.cmu.edu (R.J.).

Notes

The authors declare no competing financial interest.

ACKNOWLEDGMENTS

C.Y. acknowledges the scholarship support from the China Scholarship Council (2011836054). This work is financially supported by the U.S. Department of Energy, Office of Basic Energy Sciences (Grant DE-FG02-12ER16354), the National Natural Science Foundation of China (No. 21067004, 21263005), the Young scientists cultivating object program of Jiangxi Province (20122BCB23015), and the Jiangxi Province Education Department of Science and Technology Project (No. GJJ12344). We thank Dr. Yu Lei for assistance in STEM imaging of $Au_{25}(SR)_{18}/TiO_2$ catalysts.

REFERENCES

(1) Teranishi, M.; Naya, S.; Tada, H. In Situ Liquid Phase Synthesis of Hydrogen Peroxide from Molecular Oxygen Using Gold Nanoparticle-Loaded Titanium (IV) Dioxide Photocatalyst. *J. Am. Chem. Soc.* **2010**, *132*, 7850−7851.

(2) Wang, X. D.; Blackford, M.; Prince, K.; Caruso, R. A. Preparation of Boron-Doped Porous Titania Networks Containing Gold Nanoparticles with Enhanced Visible-Light Photocatalytic Activity. *ACS Appl. Mater. Interfaces* **2012**, *4*, 476−482.

(3) Primo, A.; Marino, T.; Corma, A.; Molinari, R.; García, H. Efficient Visible-Light Photocatalytic Water Splitting by Minute Amounts of Gold Supported on Nanoparticulate CeO_2 Obtained by a Biopolymer Templating Method. *J. Am. Chem. Soc.* **2011**, *133*, 6930−6933.

(4) Lee, J.; Mubeen, S.; Ji, X. L; Stucky, G. D.; Moskovits, M. Plasmonic Photoanodes for Solar Water Splitting with Visible Light. *Nano Lett.* **2012**, *12*, 5014−5019.

(5) Wang, F.; Li, C. H.; Chen, H. J.; Jiang, R. B.; Sun, L. D.; Li, Q.; Wang, J. F.; Yu, J. C.; Yan, C. H. Plasmonic Harvesting of Light Energy for Suzuki Coupling Reactions. *J. Am. Chem. Soc.* **2013**, *135*, 5588−5601.

(6) Sarina, S.; Zhu, H.; Jaatinen, E.; Xiao, Q.; Liu, H. W.; Jia, J. F.; Chen, C.; Zhao, J. Enhancing Catalytic Performance of Palladium in Gold and Palladium Alloy Nanoparticles for Organic Synthesis Reactions through Visible Light Irradiation at Ambient Temperatures. *J. Am. Chem. Soc.* **2013**, *135*, 5793−5801.

(7) Kelly, K. L.; Coronado, E.; Zhao, L. L.; Schatz, G. C. The Optical Properties of Metal Nanoparticles: the Influence of Size, Shape, and Dielectric Environment. *J. Phys. Chem. B* **2003**, *107*, 668−677.
(8) Torimoto, T.; Horibe, H.; Kameyama, T.; Okazaki, K.; Ikeda, S.; Matsumura, M.; Ishikawa, A.; Ishihara, H. Plasmon-Enhanced Photocatalytic Activity of Cadmium Sulfide Nanoparticle Immobilized on Silica-Coated Gold Particles. *J. Phys. Chem. Lett.* **2011**, *2*, 2057−2062.
(9) Zhou, X. M.; Liu, G.; Yu, J. G.; Fan, W. H. Surface Plasmon Resonance-Mediated Photocatalysis by Noble Metal-Based Composites under Visible Light. *J. Mater. Chem.* **2012**, *22*, 21337−21354.
(10) Tian, Y.; Tatsuma, T. Mechanisms and Applications of Plasmon-Induced Charge Separation at TiO_2 Films Loaded with Gold Nanoparticles. *J. Am. Chem. Soc.* **2005**, *127*, 7632−7637.
(11) Kowalska, E.; Abe, R.; Ohtani, B. Visible Light-Induced Photocatalytic Reaction of Gold-Modified Titanium (IV) Oxide Particles: Action Spectrum Analysis. *Chem. Commun.* **2009**, 241−243.
(12) Qian, H.; Zhu, M.; Wu, Z.; Jin, R. Quantum Sized Gold Nanoclusters with Atomic Precision. *Acc. Chem. Res.* **2012**, *45*, 1470−1479.
(13) Zhu, M.; Aikens, C. M.; Hollander, F. J.; Schatz, G. C.; Jin, R. Correlating the Crystal Structure of a Thiol-Protected Au_{25} Cluster and Optical Properties. *J. Am. Chem. Soc.* **2008**, *130*, 5883−5885.
(14) Qian, H. F.; Eckenhoff, W. T.; Zhu, Y.; Pintauer, T.; Jin, R. C. Total Structure Determination of Thiolate-Protected Au_{38} Nanoparticles. *J. Am. Chem. Soc.* **2010**, *132*, 8280−8281.
(15) Wu, Z.; Jin, R. On the Ligand's Role in the Fluorescence of Gold Nanoclusters. *Nano Lett.* **2010**, *10*, 2568−2573.
(16) Devadas, M. S.; Kim, J.; Sinn, E.; Lee, D.; Goodson, T., III; Ramakrishna, G. Unique Ultrafast Visible Luminescence in Monolayer-Protected Au_{25} Clusters. *J. Phys. Chem. C* **2010**, *114*, 22417−22423.
(17) Shichibu, Y.; Negishi, Y.; Tsunoyama, H.; Kanehara, M.; Teranishi, T.; Tsukuda, T. Extremely High Stability of Glutathionate-Protected Au_{25} Clusters against Core Etching. *Small* **2007**, *3*, 835−839.
(18) Chen, Y. S.; Choi, H.; Kamat, P. V. Metal Cluster Sensitized Solar Cells. A New Class of Thiolated Gold Sensitizers Delivering Efficiency Greater than 2%. *J. Am. Chem. Soc.* **2013**, *135*, 8822−8825.
(19) Devadas, M. S.; Kwak, K.; Park, J. W.; Choi, J. H.; Jun, C. H.; Sinn, E.; Ramakrishna, G.; Lee, D. Directional Electron Transfer in Chromophore-Labeled Quantum-Sized Au_{25} Clusters: Au_{25} as an Electron Donor. *J. Phys. Chem. Lett.* **2010**, *1*, 1497−1503.
(20) Kogo, A.; Sakai, N.; Tatsuma, T. Photocatalysis of Au_{25}-Modified TiO_2 under Visible and Near Infrared Light. *Electrochem. Commun.* **2010**, *12*, 996−999.
(21) Kogo, A.; Sakai, N.; Tatsuma, T. Photoelectrochemical Analysis of Size-Dependent Electronic Structures of Gold Clusters Supported on TiO_2. *Nanoscale* **2012**, *4*, 4217−4221.
(22) Lee, J.; Shim, H. S.; Lee, M.; Song, J. K.; Lee, D. Size-Controlled Electron Transfer and Photocatalytic Activity of ZnO−Au Nanoparticle Composites. *J. Phys. Chem. Lett.* **2011**, *2*, 2840−2845.
(23) Li, G.; Jin, R. Atomically Precise Gold Nanoclusters as New Model Catalysts. *Acc. Chem. Res.* **2013**, DOI: 10.1021/ar300213z.
(24) Li, G.; Qian, H.; Jin, R. Gold Nanocluster-Catalyzed Selective Oxidation of Sulfide to Sulfoxide. *Nanoscale* **2012**, *4*, 6714−6717.
(25) Nie, X.; Qian, H.; Ge, Q.; Xu, H.; Jin, R. CO Oxidation Catalyzed by Oxide-Supported $Au_{25}(SR)_{18}$ Nanoclusters and Identification of Perimeter Sites as Active Centers. *ACS Nano* **2012**, *6*, 6014−6022.
(26) Petrik, N. G.; Kimmel, G. A. Oxygen Photochemistry on TiO_2 (110): Recyclable, Photoactive Oxygen Produced by Annealing Adsorbed O_2. *J. Phys. Chem. Lett.* **2011**, *2*, 2790−2796.
(27) Hoffmann, M. R.; Martin, S. T.; Choi, W.; Bahnemann, D. W. Environmental Applications of Semiconductor Photocatalysis. *Chem. Rev.* **1995**, *95*, 69−96.
(28) Yu, C. L.; Fan, Q. Z.; Xie, Y.; Chen, J. C.; Shu, Q.; Yu, J. C. Sonochemical Fabrication of Novel Square-Shaped F Doped TiO_2 Nanocrystals with Enhanced Performance in Photocatalytic Degradation of Phenol. *J. Hazard. Mater.* **2012**, *38/45*, 237−238.
(29) Liu, S. W.; Yu, J. G.; Jaroniec, M. Tunable Photocatalytic Selectivity of Hollow TiO_2 Microspheres Composed of Anatase Polyhedra with Exposed {001} Facets. *J. Am. Chem. Soc.* **2010**, *132*, 11914−11916.
(30) Xiang, Q. J.; Yu, J. G.; Jaroniec, M. Synergetic Effect of MoS_2 and Graphene as Cocatalysts for Enhanced Photocatalytic H_2 Production Activity of TiO_2 Nanoparticles. *J. Am. Chem. Soc.* **2012**, *134*, 6575−6578.
(31) Sun, F. Q.; Yu, J. C.; Wang, X. C. Construction of Size-Controllable Hierarchical Nanoporous TiO_2 Ring Arrays and Their Modifications. *Chem. Mater.* **2006**, *18*, 3774−3779.
(32) Zhu, M.; Eckenhoff, W. T.; Pintauer, T.; Jin, R. Conversion of Anionic $[Au_{25}(SCH_2CH_2Ph)_{18}]^-$ Cluster to Charge Neutral Cluster via Air Oxidation. *J. Phys. Chem. C* **2008**, *112*, 14221−14224.
(33) Wu, Z.; Chen, J.; Jin, R. One-Pot Synthesis of $Au_{25}(SG)_{18}$, 2 and 4 nm Gold Nanoparticles and Comparison of Their Size-Dependent Properties. *Adv. Funct. Mater.* **2011**, *21*, 177−183.
(34) Donkers, R. L.; Lee, D.; Murray, R. W. Synthesis and Isolation of the Molecule-Like Cluster $Au_{38}(PhCH_2CH_2S)_{24}$. *Langmuir* **2004**, *20*, 1945−1952.
(35) Tracy, J. B.; Kalyuzhny, G.; Crowe, M. C.; Balasubramanian, R.; Choi, J. P.; Murray, R. W. Poly(ethylene glycol) Ligands for High-Resolution Nanoparticle Mass Spectrometry. *J. Am. Chem. Soc.* **2007**, *129*, 6706−6707.
(36) Shichibu, Y.; Negishi, Y.; Tsukuda, T.; Teranishi, T. Large-Scale Synthesis of Thiolated Au_{25} Clusters via Ligand Exchange Reactions of Phosphine-Stabilized Au_{11} Clusters. *J. Am. Chem. Soc.* **2005**, *127*, 13464−13465.
(37) Vinodgopal, K.; Wynkoop, D. E.; Kamat, P. V. Environmental Photochemistry on Semiconductor Surfaces: Photosensitized Degradation of a Textile Azo Dye, Acid Orange 7, on TiO_2 Particles Using Visible Light. *Environ. Sci. Technol.* **1996**, *30*, 1660−1666.
(38) Yan, X. L.; Ohno, T.; Nishijima, K.; Abe, R.; Ohtani, B. Is Methylene Blue an Appropriate Substrate for a Photocatalytic Activity Test? A Study with Visible-Light Responsive Titania. *Chem. Phys. Lett.* **2006**, *429*, 606−610.
(39) Yang, S. Y.; Chen, Y. Y.; Zheng, J. G.; Cui, Y. J. Enhanced Photocatalytic Activity of TiO_2 by Surface Fluorination in Degradation of Organic Cationic Compound. *J. Environ. Sci.* **2007**, *19*, 86−89.
(40) Yu, C. L.; Yu, J. C.; Chan, M. Sonochemical Fabrication of Fluorinated Mesoporous Titanium Dioxide Microspheres. *J. Solid State Chem.* **2009**, *182*, 1061−1069.
(41) Hufschmidt, D.; Liu, L.; Seizer, V. Photocatalytic Water Treatment: Fundamental Knowledge Required for Its Practical Application. *Water Sci. Technol.* **2004**, *49*, 135−140.
(42) Wang, S. Z.; Gao, R. M; Zhou, F. M.; Selke, M. Nanomaterials and Singlet Oxygen Photosensitizers: Potential Applications in Photodynamic Therapy. *J. Mater. Chem.* **2004**, *14*, 487−493.